

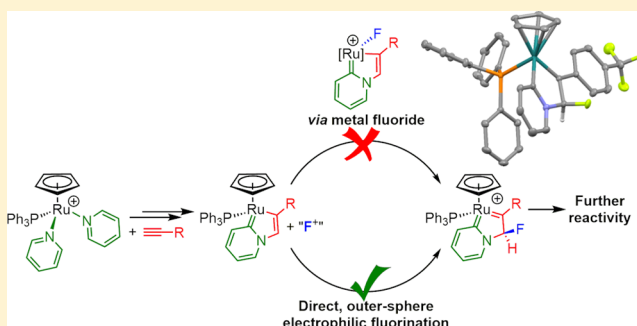
Outer-Sphere Electrophilic Fluorination of Organometallic Complexes

Lucy M. Milner, Natalie E. Pridmore, Adrian C. Whitwood, Jason M. Lynam,* and John M. Slattery*

Department of Chemistry, University of York, Heslington, York YO10 SDD, United Kingdom

Supporting Information

ABSTRACT: Organofluorine chemistry plays a key role in materials science, pharmaceuticals, agrochemicals, and medical imaging. However, the formation of new carbon–fluorine bonds with controlled regiochemistry and functional group tolerance is synthetically challenging. The use of metal complexes to promote fluorination reactions is of great current interest, but even state-of-the-art approaches are limited in their substrate scope, often require activated substrates, or do not allow access to desirable functionality, such as alkenyl C(sp²)–F or chiral C(sp³)–F centers. Here, we report the formation of new alkenyl and alkyl C–F bonds in the coordination sphere of ruthenium via an unprecedented outer-sphere electrophilic fluorination mechanism. The organometallic species involved are derived from nonactivated substrates (pyridine and terminal alkynes), and C–F bond formation occurs with full regio- and diastereoselectivity. The fluorinated ligands that are formed are retained at the metal, which allows subsequent metal-mediated reactivity.



INTRODUCTION

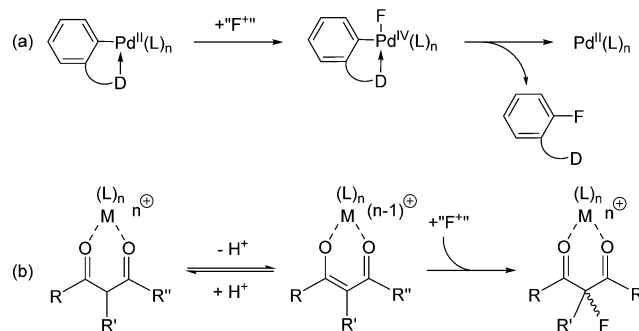
Fluorine-containing organic molecules are found in a wide range of applications from liquid crystals to blockbuster drugs such as fluoxetine and atorvastatin but are of particular interest in pharmaceuticals,¹ agrochemicals, and medical imaging.^{2,3} The unique properties of C–F bonds, which can improve metabolic stability, bioavailability, and lipophilicity, mean that around 30% of all agrochemicals and 20% of all pharmaceuticals now contain fluorine.⁴ In addition, the use of ¹⁸F-labeled compounds in positron emission tomography (PET) is a highly active and important area of medical imaging research.⁵ As such, there is a synthetic requirement to develop simple and efficient (and in the case of ¹⁸F labeling, where the ¹⁸F half-life is short, rapid) methods for the introduction of fluorine into organic molecules.

Selective formation of new carbon–fluorine bonds, particularly in the presence of sensitive functional groups, is synthetically challenging.⁵ In addition to organocatalytic and photocatalytic C–F bond formation,^{5–11} enzymatic C–F bond formation,¹² and the use of metal complexes to produce new fluorinated building blocks by selective C–F activation,^{13,14} there has been a major focus in recent years on the development of new transition-metal-mediated C–F bond-forming reactions, which offer significant potential for regioselectivity and atom- and step-economy under mild conditions. There have recently been some significant advances in metal-catalyzed fluorination using fluoride salts as the fluorine source.^{5,15–24} However, fluoride salts are not always ideal for the introduction of fluorine into organic molecules, particularly those with sensitive functional groups, as the

nucleophilicity and basicity of F[–] can result in unwanted side reactions.

To circumvent these problems, a number of metal-catalyzed electrophilic fluorination reactions have been developed, where C–F bonds are formed from latent sources of “F⁺”.^{5,25–30} These reactions can typically be divided into two key mechanistic classes (e.g., Scheme 1). In the first, reaction of a redox-active metal complex with F⁺ leads to initial metal–

Scheme 1. Examples of Some Transition-Metal-Mediated Electrophilic Fluorination Mechanisms^a



^aConditions: (a) Aryl C–H fluorination via reductive elimination from a Pd(IV) intermediate. D = donor group, e.g., pyridyl; L = ligand. (b) Lewis-acid-mediated C–F bond formation via stabilized carbanion. M = e.g. Ti, Ru; L = ligand.⁵

Received: June 24, 2015

Published: August 13, 2015



fluoride bond formation, with concomitant oxidation of the metal. The high oxidation state of the metal (potentially assisted by ligand dissociation or by formation of multimetallic species)^{31–34} then facilitates C–F reductive elimination. Alternatively, the redox-active metal may initiate one-electron transfer processes that promote subsequent radical reactions.³⁵ In the second class, Lewis acidic metals are used to stabilize carbanionic nucleophiles, which react with F⁺ without any redox chemistry occurring at the metal. Cu^{II}, Ni^{II}, Zn^{II}, Ti^{IV}, and even Pd^{II} and Ru^{II} have been used in this way to stabilize anions derived from β -ketocarbonyl compounds during C(sp³)–F bond-forming reactions.⁵

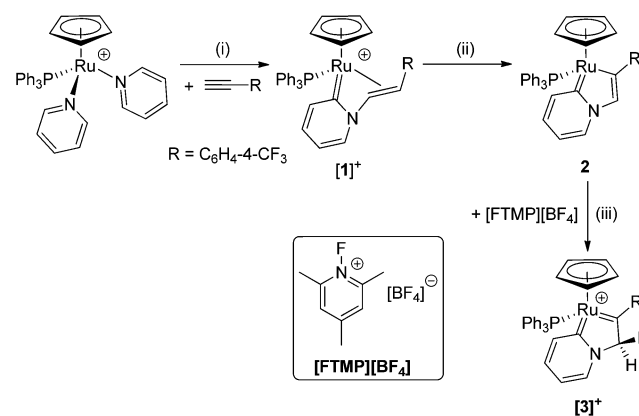
These are powerful strategies that are broadly applicable, but there are some limitations. For example, in Pd-catalyzed C–H fluorination reactions, directing groups (e.g., pyridyl, amino, *N*-perfluorotolylamide groups) are required to provide regioselectivity.^{36–39} In other cases, preactivation of the substrate (for example, by formation of an aryl stannane, silane, or boronic acid) is required to promote the reaction.^{28,34,38,40–42} In addition, recent developments have often focused on aryl C–F bond formation.⁴³ Those metal-mediated electrophilic C(sp³)–F forming reactions that have been developed typically require highly activated substrates (e.g., β -ketocarbonyl compounds such as β -diketones, β -keto esters, or *N*-Boc-protected amides),⁵ which reduces potential substrate scope. As such, the development of new organometallic reactivity that may lead to new regio- and stereoselective metal-mediated electrophilic fluorination reactions, without the need for directing and/or activating groups, is of great interest. Reactions that allow the construction of less common structural frameworks, for example, those containing alkenyl or alkyl C–F bonds (especially chiral C(sp³)–F centers) are particularly interesting.

This paper describes the formation of new alkenyl and alkyl C–F bonds in the coordination sphere of ruthenium via an unprecedented outer-sphere electrophilic fluorination (OSEF) mechanism. The ruthenium-containing organometallic species involved are derived from substrates that are not prefunctionalized (i.e., pyridine and terminal alkynes), and C–F bond formation occurs with complete regio- and diastereoselectivity. Crucially, the fluorinated ligands that are formed are retained in the coordination sphere of the metal, which allows subsequent metal-mediated reactivity after the electrophilic fluorination step. In a related study, we have recently shown that OSEF processes can also be used to generate the first examples of mononuclear fluorovinylidene complexes, which demonstrates that a range of substrates are susceptible to this reactivity.⁴⁴ Incorporation of this novel mechanism of fluorination into stoichiometric or catalytic synthetic methodologies has the potential to expand the range of fluorinated molecules available via metal-mediated fluorination.

RESULTS

It has recently been shown that novel vinyl pyridylidene ([1][PF₆]) and 1-ruthanaindolizine (2) complexes can be formed under mild conditions by ruthenium-mediated C–H functionalization of pyridine (Scheme 2).⁴⁵ We report here the use of these organometallic species to develop a simple and selective method to promote C–F bond formation in the coordination sphere of ruthenium. Treatment of 2 with a stoichiometric quantity of 1-fluoro-2,4,6-trimethylpyridinium tetrafluoroborate ([FTMP][BF₄]), as a latent source of F⁺, resulted in the quantitative (by NMR) conversion of 2 to a new, bright-green complex characterized by single ³¹P{¹H}

Scheme 2. Reaction of [CpRu(PPh₃)(Pyr)₂][PF₆] with Terminal Alkynes and Subsequent Fluorination^a



^aConditions: (i) CH₂Cl₂, 50 °C, 15 h; (ii) + 1,4-diazabicyclo[2.2.2]octane (DABCO), – [HDABCO]PF₆, CH₂Cl₂, 20 °C, 16 h; (iii) CH₂Cl₂, 20 °C, 20 min.

(47.2 ppm, ⁴J_{PF} = 7.7 Hz) and η^5 -C₅H₅ ¹H (5.37 ppm) resonances. The product also displayed a ¹⁹F resonance with a large HF coupling at –139.8 ppm (²J_{HF} = 52.0 Hz, ⁴J_{PF} = 7.7 Hz). HR-ESI-MS showed the presence of a cationic molecular ion at 696.1023 *m/z*, which is consistent with monofluorination of 2. These data, supported by X-ray crystallographic studies, showed that electrophilic fluorination of 2 had occurred at the 3-position on the 1-ruthanaindolizine ring, leading to the formation of complex [3][BF₄] (Scheme 2). This reactivity appears to be insensitive to the source of F⁺, with the same product being observed when 2 is reacted with Selectfluor or *N*-fluorobenzenesulfonimide (NFSI).

Single-crystal X-ray diffraction studies showed the molecular structure of [3][BF₄] (Figure 1) to contain a metallocyclic ring system similar to that seen in 2, but with the formation of a new C–F bond at C(11). The Ru–C(6) bond in [3][BF₄] has a length similar to that in 2 (1.990(2) compared to 1.996(2) Å), whereas the Ru–C(12) bond is significantly shorter (1.916(2)

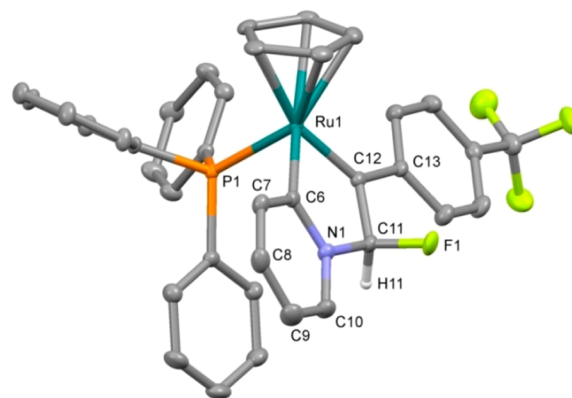


Figure 1. Solid-state structure of [3][BF₄], monoclinic *P*2₁. Thermal ellipsoids are shown at the 50% level. Hydrogen atoms {except for H(11)} and the [BF₄][–] counterion are omitted for clarity. Selected bond lengths (Å) and angles (deg): Ru(1)–C(6) = 1.990(2), Ru(1)–C(12) = 1.916(2), Ru(1)–P(1) = 2.3238(5), C(12)–C(11) = 1.508(3), C(11)–N(1) = 1.436(3), N(1)–C(6) = 1.368(2), C(11)–F(1) = 1.403(2), C(12)–C(11)–F(1) = 108.5(2), C(12)–C(11)–H(11) = 117.7(1), C(12)–C(11)–N(1) = 109.9(2), N(1)–C(11)–H(11) = 106.7(1).

compared to 2.046(2) Å), consistent with an increase in double bond character upon fluorination. The C(11)–C(12) bond is elongated in [3][BF₄] compared to 2 (1.508(3) vs 1.339(2) Å), which is consistent with the formal loss of double bond character.

Overall the most appropriate Lewis structure for [3]⁺ appears to be that shown in Scheme 2, which invokes pyridylidene (rather than pyridyl) character to the Ru–C(6) bond and Schrock-type carbene character to C(12). This is supported by NBO analysis (see Supporting Information for details). As discussed previously for [1]⁺ and 2,⁴⁵ there is considerable π character to the Ru–C(6) bond in [3]⁺, modeled in the NBO analysis as donation of metal-based electron density to a C(6)–N(1) π^* orbital (occupation = 0.483e[−]; stabilization energy = 83 kJ mol^{−1}). This interaction is π -bonding with respect to Ru–C(6). The Ru–C(12) bond in [3]⁺ is a double bond in the NBO reference structure (π -bond occupancy = 1.815e[−]), and its Wiberg bond index is significantly larger than the equivalent Ru–C bond in 2 (1.067 vs 0.665), consistent with significant Ru–C(12) multiple bond character. The nature of the different carbene ligands is also reflected in the ¹³C{¹H} NMR spectrum, in which C(6) exhibits a resonance at δ 211.8 and C(12) at δ 301.4, consistent with a nitrogen-containing Fischer carbene and a Schrock carbene, respectively.⁴⁶

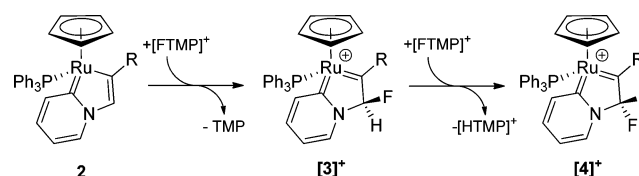
Based on this Lewis structure, Ru can be considered to have a formal oxidation state of +4 with one Fischer-type and one Schrock-type carbene ligand present. As such, the electrophilic fluorination reaction observed here is distinctly different from other previously reported metal-mediated electrophilic fluorination reactions. It is oxidative (with regard to the metal), which is similar to related Pd chemistry, but different to non-redox electrophilic fluorination reactions promoted by Lewis acidic metals (e.g., Ti).⁵ However, unlike in the Pd cases, the reaction produces an outer-sphere fluorination product, which we believe occurs without the involvement of a Ru–F intermediate (vide infra).

Fluorination of the 3-position on the 1-ruthanaindolizine ring in racemic 2 leads to the creation of a new stereogenic carbon center C(11) in [3][BF₄]. The reaction is diastereoselective, leading only to the diastereomer in which the C–F bond points toward the C₅H₅ ring. This is supported by NOESY experiments that show no cross-peak between H(11) and the hydrogen atoms of the C₅H₅ ring. The single-crystal X-ray structure of [3][BF₄] is enantiopure, containing only the RR enantiomer. This diastereoselectivity is driven by steric effects: F⁺ addition to the “inside” face of the 1-ruthanaindolizine ring is blocked by the three Ph groups on the phosphine. This is likely to be a kinetic, rather than thermodynamic, effect as the products of F⁺ addition to the two faces are found to be essentially isoenergetic (−194 and −192 kJ mol^{−1} for the “outside” and “inside” faces, respectively, relative to 2 and [FTMP]⁺) in DFT studies (vide infra). The geometry around C(11) is slightly distorted from ideal tetrahedral geometry, and the C(11)–F(1) bond length is rather long for a typical sp³-hybridized C–F bond at 1.403(2) Å.

Further Reactivity of [3][BF₄]. Interestingly, [3][BF₄] is susceptible to further electrophilic fluorination. When 2 equiv of [FTMP][BF₄] are added to 2 in dichloromethane, [3][BF₄] is observed to form immediately in the NMR spectra, and over a period of 24 h, this species converts cleanly to a new complex [4][BF₄]. The characteristic ¹⁹F resonance for F(1) of [3][BF₄], observed at −139.8 ppm (dd, ²J_{HF} = 52.0 Hz, ⁴J_{PF} = 7.7 Hz), is replaced by two ¹⁹F resonances at −98.3 (d, ²J_{FF} =

233.1 Hz) and −79.7 (dd, ²J_{FF} = 233.1 Hz, ⁴J_{PF} = 6.6 Hz) ppm, which are strongly mutually coupled. HR-ESI-MS showed the presence of a cationic molecular ion at 714.0920 *m/z*, which indicated that net deprotono-difluorination of 2 had occurred. The spectroscopic data and a subsequent single-crystal X-ray diffraction study showed that geminal deprotono-difluorination of the 3-position on the 1-ruthanaindolizine ring in 2 had taken place (Scheme 3). This appears to occur as a two-stage process

Scheme 3. Reaction of 2 with Two Equivalents of [FTMP][BF₄]^a



^aConditions: + 2 equiv of [FTMP][BF₄], − NC₅H₂Me₃, − [HTMP][BF₄], CH₂Cl₂, 20 °C, 24 h.

via formal F⁺ addition to give [3][BF₄] and subsequent C–H activation (presumably via deprotonation of [3][BF₄] by free 2,4,6-trimethylpyridine (TMP) in the reaction mixture) and fluorination to give [4][BF₄]. Indeed, reaction of isolated [3][BF₄] with [FTMP][BF₄], which contains traces of free TMP, does afford [4][BF₄] in a quantitative fashion.

The molecular structure of [4][BF₄] (Figure 2) displays metric parameters similar to those of [3][BF₄], with a Ru–

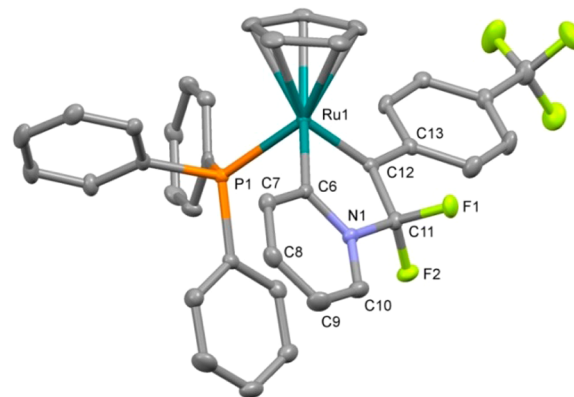


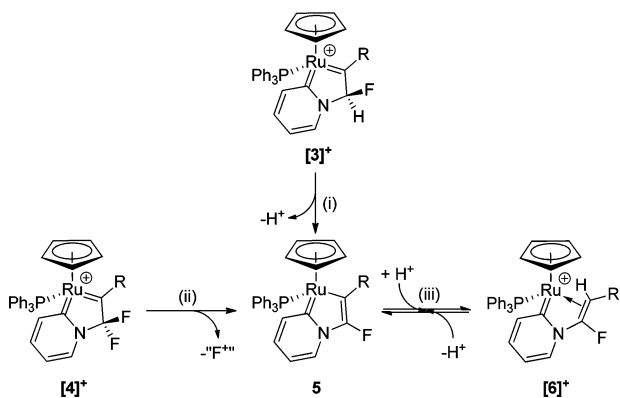
Figure 2. Solid-state structure of [4][BF₄], monoclinic *Cc*. Thermal ellipsoids are shown at the 50% level. Hydrogen atoms and the [BF₄][−] counterion are omitted for clarity. Selected bond lengths (Å) and angles (deg): Ru(1)–C(6) = 2.010(3), Ru(1)–C(12) = 1.902(3), Ru(1)–P(1) = 2.3585(6), C(12)–C(11) = 1.516(4), C(11)–N(1) = 1.459(3), N(1)–C(6) = 1.374(3), C(11)–F(1) = 1.374(3), C(11)–F(2) = 1.353(3), C(12)–C(11)–F(1) = 111.2(2), C(12)–C(11)–F(2) = 115.6(2), C(12)–C(11)–N(1) = 109.4(2), N(1)–C(11)–F(2) = 109.0(2).

C(6) distance {2.010(3) Å} that is similar to that in the parent metallocycle, 2, but with a significantly shorter Ru–C(12) distance {1.902(3) Å} compared to that in 2. As with [3][BF₄], this suggests some pyridylidene character at C(6) and significant Schrock-type carbene character at C(12), and both fluorinated products can be described by similar Lewis structures. The C–F bond lengths of C(11)–F(1) {1.374(3) Å} and C(11)–F(2) {1.353(3) Å} in [4][BF₄] are significantly shorter than those in [3][BF₄] and are more similar to typical

sp^3 C–F bond lengths, with slightly less distortion around C(11) from ideal tetrahedral angles.

The 1-ruthana-3-fluoroindolizine complex **5**, which is presumed to be an intermediate in the formation of $[4][BF_4]$ from $[3][BF_4]$, can be formed by deprotonation of $[3][BF_4]$ with 1,4-diazabicyclo[2.2.2]octane (DABCO) in CH_2Cl_2 (Scheme 4). This results in the formal reduction of the metal

Scheme 4. Further Reactivity of $[3][BF_4]$ and $[4][BF_4]$ ^a



^aConditions: (i) pyridine-*d*₅, 20 °C; or + DABCO, – [H-DABCO]·[BF₄], CD₂Cl₂, 20 °C; (ii) pyridine-*d*₅, 20 °C, 7 days; (iii) equilibrium in the presence of [H-DABCO][BF₄] in CD₂Cl₂, 20 °C.

from Ru +4 in $[3]^+$ to Ru +2 in **5**. In the presence of [H-DABCO][BF₄] in CH_2Cl_2 , **5** is in equilibrium with a new α -fluorovinyl pyridylidene complex $[6][BF_4]$ and free DABCO, which results in dynamic behavior that is rapid on the NMR time scale at room temperature. Cooling this mixture to 195 K

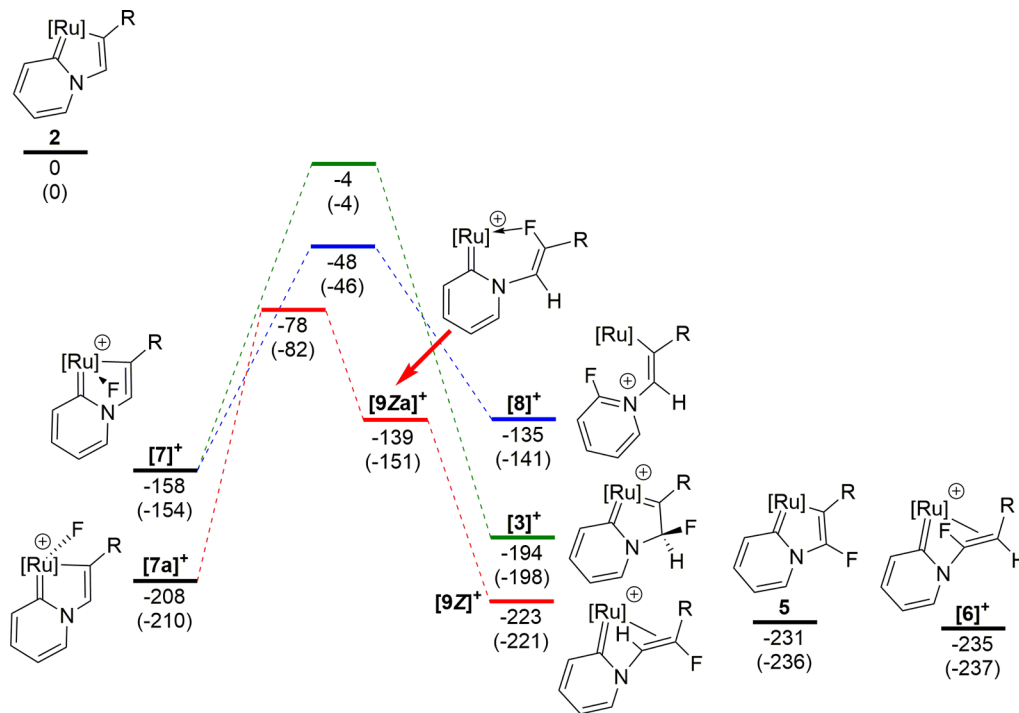
was not sufficient to freeze out all dynamic behavior, but broad signals at ¹⁹F δ = –112 ppm and ³¹P δ = 62 ppm associated with **5** can clearly be seen. Similar dynamic behavior has been observed for **2**.⁴⁵ In order to prepare a sample of **5** that was free from this dynamic behavior, $[3][BF_4]$ was dissolved in pyridine-*d*₅, which acts as both a base and a solvent. In this case, the presence of excess base clearly led to the formation of **5** (¹⁹F δ = –111.7 ppm and ³¹P δ = 61.5 ppm), with no evidence of dynamic behavior on the NMR time scale, which allowed full spectroscopic characterization of **5** (see Supporting Information).

Intriguingly, dissolution of $[4][BF_4]$ in pyridine-*d*₅ at room temperature also led to the formation of **5** (as the major, but not only, product) albeit slowly over the course of a week. Formation of **5** from $[4][BF_4]$ is a very unusual observation, as it appears that F⁺ has formally been lost from a C–F bond in $[4][BF_4]$ to form the 1-ruthana-3-fluoroindolizine ring of **5**. However, the spectroscopic data do not suggest that F⁺ is simply transferred to pyridine, in analogy to the loss of H⁺ from $[3][BF_4]$, as [F-NC₅H₅]⁺ was not observed. This surprising reactivity may, in fact, be linked to the formation of additional ruthenium-containing species during this reaction, which we have been unable to characterize unambiguously.

DISCUSSION

It was perhaps surprising, considering related Pd-based chemistry,³² that **2** does not appear to react with [FTMP][BF₄] via oxidative fluorination of the metal to form a Ru–F-containing species, such as $[7][BF_4]$ or $[7a][BF_4]$, or an aryl fluoride $[8][BF_4]$ via reductive elimination from a Ru–F intermediate (Scheme 5). The reactivity of **2** toward F⁺ is also very different from the reactivity of **2** toward H⁺ (which leads

Scheme 5. Potential Energy Surface for the Electrophilic Fluorination Reactions Observed^a



^aAll data are at the PBE0-D3/def2-TZVPP//BP86/SV(P) level with solvation corrections applied in CH_2Cl_2 (COSMO, ϵ = 8.93 for CH_2Cl_2 at 25 °C). $E_{SCF+ZPE}$ energies (relative to **2** and [FTMP]⁺) are shown below each state, and Gibbs energies at 298.15 K are given in brackets below these. [Ru] = [Ru(η^5 -C₅H₅)(PPh₃)], R = C₆H₄-4-CF₃; [FTMP]⁺, [HTMP]⁺ and TMP are omitted from the scheme where necessary for clarity.

to the regeneration of **1**, Scheme 2).⁴⁵ If analogous reactivity were to be seen, then this would lead to the formation of the β -fluorovinyl pyridylidene complex $[9][BF_4]$ (Scheme 5), which was also not observed. These observations suggested that electrophilic fluorination in this system is underpinned by a novel fluorination mechanism.

During the reactions above, no Ru–F intermediates, which would be expected to exhibit significantly upfield ¹⁹F chemical shifts of around –200 to –450 ppm,^{47–50} were observed spectroscopically. In order to investigate the possibility that a short-lived Ru–F intermediate was involved in the formation of $[3][BF_4]$, we undertook a low-temperature NMR study on the reaction and have probed the system using DFT studies. In the NMR study, **2** and $[FTMP][BF_4]$ were combined in CD₂Cl₂ at 195 K and introduced to a precooled NMR spectrometer at 195 K. ¹H, ³¹P, and ¹⁹F spectra were recorded as the spectrometer temperature was warmed to 295 K. The reaction appears not to proceed at temperatures below 245 K, but at 265 K, the reaction is essentially complete, suggesting relatively fast kinetics even at low temperatures. No potential reaction intermediates (Ru–F-containing species or others) were observed at any temperature during these studies, which suggested that fluorine is either directly transferred to the site of fluorination or that only low-energy transition states connect any potential intermediates to the reaction product $[3][BF_4]$.

The mechanistic features of electrophilic fluorination reactions involving F⁺ sources such as $[FTMP][BF_4]$ or Selectfluor are a matter of some debate,⁵¹ and either single-electron transfer (SET) followed by rapid radical recombination or nucleophilic attack of the substrate on the F⁺ source seem likely to occur in different systems. It is challenging to distinguish between these two mechanisms both experimentally and computationally,^{35,52} in particular, due to the difficulty in correctly describing the singlet diradical that is formed during a SET mechanism. However, our DFT studies support the suggestion that the formation of $[3][BF_4]$ does not proceed via a Ru–F complex and that direct fluorination of **2** is likely to be a low-energy process.

It can be seen from Scheme 5 that the formation of Ru–F-containing ions $[7]^+$ and $[7a]^+$ is thermodynamically favored over **2** and $[FTMP]^+$ (by 158 and 208 kJ mol^{–1}, respectively). As such, the fact that a Ru–F species is not observed is likely to be a kinetic effect. The observed product $[3]^+$ is neither the kinetic nor the thermodynamic product of F⁺ migration from such a Ru–F species to a carbon atom on the metallocycle. The kinetic and thermodynamic product is the unobserved complex $[9Z]^+$, where the 2-position of the ruthanindolizine is fluorinated. Complexes $[3]^+$, $[8]^+$, and $[9Z]^+$ are all separated from a ruthenium fluoride by significant energetic barriers (with transition states lying 204, 160, and 130 kJ mol^{–1} higher in energy than $[7a]^+$, respectively). We assume here that both Ru–F isomers are accessible and that the lowest energy isomer $[7a]^+$ will be populated. These large barriers suggest that if a Ru–F intermediate were formed under the fluorination conditions, then it would have sufficient stability to be observed as an intermediate in the low-temperature NMR experiments. In addition, a barrier of 204 kJ mol^{–1} is not consistent with the rapid formation of $[3]^+$ at 265 K, as seen in the low-temperature NMR studies. This suggests that $[3]^+$ is unlikely to be formed from $[7a]^+$ via this mechanism. The potential energy surface (PES) for the formation of the deprotonated difluorination product $[4]^+$ from a Ru–F-containing intermediate (see Supporting Information for details) is similar to that shown

in Scheme 5, which suggests that this reaction also does not proceed via a Ru–F intermediate.

Direct fluorination of the 3-position of the ruthanindolizine ring in **2** by $[FTMP]^+$ was investigated using relaxed PES scans (at the (RI-)PBE0/def2-TZVPP//((RI-)PBE0/SV(P) level) for the closed-shell singlet, triplet, and singlet diradical states (see Supporting Information for details). The reaction pathways for all states proceed via relatively low energy barriers (ΔE_{SCF}^\ddagger in CH₂Cl₂ of 58, 27, and 23 kJ mol^{–1}, respectively) to form $[3]^+$, which is consistent with the fast reaction and lack of intermediates observed experimentally. Interestingly, the open-shell pathways are found to be lower in energy than the closed-shell pathway, which suggests that a SET mechanism may operate in this system (although care should be taken in interpreting the energies of the singlet diradical states, due to spin contamination). In any event, the low barriers to fluorination directly at the ligand contrasts markedly with the large barriers for C–F bond formation via a metal–fluoride intermediate, supporting the proposal that the reaction proceeds by an outer-sphere mechanism. Fluorination at the 3-position rather than the 2-position of the ruthanindolizine ring is consistent with work by Esteruelas,⁵³ which has shown that in similar systems the 3-position is the kinetic site of protonation. Subsequent hydrogen migration to the 2-position in Esteruelas' system, to form the thermodynamic product, is presumably significantly more facile than fluorine migration in the system presented here, so $[3][BF_4]$ does not isomerize to form $[9Z][BF_4]$ under our conditions.

CONCLUSION

Reaction of the 1-ruthanindolizine complex **2** with a latent source of F⁺ results in electrophilic fluorination at the 3-position of the 1-ruthanindolizine ring to give $[3][BF_4]$. Variable-temperature NMR and DFT studies suggest that this reaction does not occur via a ruthenium–fluoride intermediate. Instead, an unprecedented direct outer-sphere electrophilic fluorination of the 3-position of the ruthanindolizine ring in **2**, potentially via a SET mechanism with a low activation energy, seems likely. This novel reactivity is distinct from previous metal-mediated electrophilic fluorination reactions, which often involve the formation of metal fluorides followed by reductive elimination or utilize non-redox-active metals to create a nucleophilic carbon center. The exploitation of OSEF reactions such as this has significant potential for the formation of new C–F bonds within the coordination sphere of an organometallic complex, with reactivity and regiochemistry that is complementary to existing methodologies. Indeed, in a related study, we have shown that mononuclear fluorovinylidene complexes, which would be challenging or impossible to prepare via conventional routes, can be synthesized using OSEF,⁴⁴ thus demonstrating the scope of this approach outside the study reported here.

EXPERIMENTAL SECTION

All air-sensitive experimental procedures were performed under an inert atmosphere of nitrogen using standard Schlenk line and glovebox techniques. Dichloromethane and pentane were purified with the aid of an Innovative Technologies anhydrous solvent engineering system. The CD₂Cl₂ and pyridine-*d*₅ used for NMR experiments was dried over CaH₂ and degassed with three freeze–pump–thaw cycles. The solvent was then transferred into NMR tubes fitted with PTFE Young's taps or stored under a nitrogen atmosphere in the glovebox. NMR spectra were acquired on a JEOL ECX-400 (operating

frequencies: 399.78 MHz for ^1H , 161.83 MHz for ^{31}P , 376.17 MHz for ^{19}F , and 100.53 MHz for ^{13}C) or a Bruker AVANCE 500 (operating frequencies: 500.13 MHz for ^1H , 202.47 MHz for ^{31}P , and 125.77 MHz for ^{13}C). ^{31}P and ^{13}C spectra were recorded with proton decoupling. Assignments were confirmed with the aid of 2D-COSY, NOESY, HMQC, and HMBC experiments. Mass spectra were recorded on a Bruker micrOTOF using electrospray ionization. Crystallographic data for [3][BF₄] and [4][BF₄] have been deposited with the Cambridge Crystallographic Data Centre under deposition numbers CCDC 1401249 and CCDC 1401248, respectively.

Calculations were performed at the (RI)-PBE0/def2-TZVP//((RI)-BP86/SV(P) level (a methodology that we have validated in a related system)⁵⁴ with the full ligand substituents used in the experimental study using TURBOMOLE version 6.4.⁵⁵ Data presented include dichloromethane solvation (using the COSMO method with $\epsilon = 8.93$ for dichloromethane at 25 °C).⁵⁶ Single-point DFT-D3 corrections have been applied at the PBE0-D3 level (on the (RI)-BP86/SV(P) geometries) using Grimme's DFT-D3 (V3.0 Rev 2, with BJ-damping) program, and data include this correction.^{57,58} Gas-phase data are provided in the Supporting Information. Both ZPE-corrected SCF energies ($E_{\text{SCF+ZPE}}$) and Gibbs energies at 298.15 K are shown, and energies quoted are relative to **2** and [FTMP]⁺. $E_{\text{SCF+ZPE}}$ data are discussed in the main section of the article due to the difficulty in assessing entropy changes in solution from gas-phase calculations. Minima were confirmed as such by the absence of imaginary frequencies, and transition states were identified by the presence of one imaginary frequency with subsequent verification by DRC analyses.

Synthesis of [Ru($\eta^5\text{-C}_5\text{H}_5$)(PPh₃)(C₅H₄NCHFC(C₆H₄-4-CF₃))][BF₄], [3][BF₄]. An ampule was charged with Ru($\eta^5\text{-C}_5\text{H}_5$)(PPh₃)(C₅H₄NCHFC(C₆H₄CF₃)), **2** (20 mg, 30 μmol), and dichloromethane (2 mL). [FTMP][BF₄] (6.1 mg, 27 μmol) was added dropwise as a dilute solution in dichloromethane (5 mL). The solution was stirred for 40 min until the color change from brown to green was deemed complete, and the volume of solvent was reduced to 0.5 mL. The addition of excess pentane yielded a green precipitate of [3][BF₄], which was washed with additional pentane. Isolated yield = 7 mg (30%). Although the reaction is quantitative by NMR spectroscopy, the necessarily small scales used lead to mechanical losses during isolation and low isolated yields.

Synthesis of [Ru($\eta^5\text{-C}_5\text{H}_5$)(PPh₃)(C₅H₄NCF₂C(C₆H₄-4-CF₃))][BF₄], [4][BF₄]. An NMR tube with a PTFE Young's tap was charged with Ru($\eta^5\text{-C}_5\text{H}_5$)(PPh₃)(C₅H₄NCHFC(C₆H₄CF₃)), **2** (20 mg, 30 μmol), and [FTMP][BF₄] (13.6 mg, 60 μmol) in CD₂Cl₂ (0.5 mL) and allowed to stand for 24 h. On complete conversion, the reaction mixture was transferred to a Schlenk tube, and the addition of excess pentane yielded a green precipitate of [4][BF₄], which was washed with additional pentane. Isolated yield = 9 mg (38%). Although the reaction is quantitative by NMR spectroscopy, the necessarily small scales used lead to mechanical losses during isolation and low isolated yields.

■ ASSOCIATED CONTENT

📄 Supporting Information

The Supporting Information is available free of charge on the ACS Publications website at DOI: 10.1021/jacs.5b06547.

X-ray data for [3][BF₄] (CIF)

X-ray data for [4][BF₄] (CIF)

Detailed experimental procedures and characterization of compounds and details of the DFT calculations, including coordinates for all species investigated (PDF)

■ AUTHOR INFORMATION

Corresponding Authors

*jason.lynam@york.ac.uk

*john.slattery@york.ac.uk

Notes

The authors declare no competing financial interest.

■ ACKNOWLEDGMENTS

We thank the EPSRC (DTA studentship to L.M.M. and computational equipment (ref. EP/H011455/1 and EP/K031589/1)) and the University of York for funding. We are very grateful to Professors Robin Perutz, Peter O'Brien, Duncan Bruce, Odile Eisenstein, and Christophe Raynaud for insightful comments on this work.

■ REFERENCES

- (1) Muller, K.; Faeh, C.; Diederich, F. *Science* **2007**, *317*, 1881.
- (2) Jeschke, P. *ChemBioChem* **2004**, *5*, 570.
- (3) Ametamey, S. M.; Honer, M.; Schubiger, P. A. *Chem. Rev.* **2008**, *108*, 1501.
- (4) Bégué, J.-P.; Bonnet-Delpon, D. *Bioorganic and Medicinal Chemistry of Fluorine*; John Wiley & Sons, Inc.: Hoboken, NJ, 2008.
- (5) Liang, T.; Neumann, C. N.; Ritter, T. *Angew. Chem., Int. Ed.* **2013**, *52*, 8214.
- (6) Rueda-Becerril, M.; Mahe, O.; Drouin, M.; Majewski, M. B.; West, J. G.; Wolf, M. O.; Sammis, G. M.; Paquin, J. F. *J. Am. Chem. Soc.* **2014**, *136*, 2637.
- (7) Bloom, S.; Knippel, J. L.; Lectka, T. *Chem. Sci.* **2014**, *5*, 1175.
- (8) Halperin, S. D.; Fan, H.; Chang, S.; Martin, R. E.; Britton, R. *Angew. Chem., Int. Ed.* **2014**, *53*, 4690.
- (9) Kee, C. W.; Chin, K. F.; Wong, M. W.; Tan, C. H. *Chem. Commun.* **2014**, *50*, 8211.
- (10) Xia, J. B.; Zhu, C.; Chen, C. *J. Am. Chem. Soc.* **2013**, *135*, 17494.
- (11) Xia, J. B.; Zhu, C.; Chen, C. *Chem. Commun.* **2014**, *50*, 11701.
- (12) O'Hagan, D.; Deng, H. *Chem. Rev.* **2015**, *115*, 634.
- (13) Ahrens, T.; Kohlmann, J.; Ahrens, M.; Braun, T. *Chem. Rev.* **2015**, *115*, 931.
- (14) Weaver, J.; Senaweera, S. *Tetrahedron* **2014**, *70*, 7413.
- (15) Wu, J. *Tetrahedron Lett.* **2014**, *55*, 4289.
- (16) Braun, M. G.; Doyle, A. G. *J. Am. Chem. Soc.* **2013**, *135*, 12990.
- (17) Braun, M. G.; Katcher, M. H.; Doyle, A. G. *Chem. Sci.* **2013**, *4*, 1216.
- (18) Dang, H.; Mailig, M.; Lalic, G. *Angew. Chem., Int. Ed.* **2014**, *53*, 6473.
- (19) Huang, X. Y.; Liu, W.; Ren, H.; Neelamegam, R.; Hooker, J. M.; Groves, J. T. *J. Am. Chem. Soc.* **2014**, *136*, 6842.
- (20) Ichiishi, N.; Canty, A. J.; Yates, B. F.; Sanford, M. S. *Org. Lett.* **2013**, *15*, 5134.
- (21) Lee, H. G.; Milner, P. J.; Buchwald, S. L. *J. Am. Chem. Soc.* **2014**, *136*, 3792.
- (22) Liu, W.; Groves, J. T. *Angew. Chem., Int. Ed.* **2013**, *52*, 6024.
- (23) Mazzotti, A. R.; Campbell, M. G.; Tang, P. P.; Murphy, J. M.; Ritter, T. *J. Am. Chem. Soc.* **2013**, *135*, 14012.
- (24) Truong, T.; Klimovica, K.; Daugulis, O. *J. Am. Chem. Soc.* **2013**, *135*, 9342.
- (25) Bloom, S.; Pitts, C. R.; Woltornist, R.; Griswold, A.; Holl, M. G.; Lectka, T. *Org. Lett.* **2013**, *15*, 1722.
- (26) Lou, S. J.; Xu, D. Q.; Xia, A. B.; Wang, Y. F.; Liu, Y. K.; Du, X. H.; Xu, Z. Y. *Chem. Commun.* **2013**, *49*, 6218.
- (27) Lou, S. J.; Xu, D. Q.; Xu, Z. Y. *Angew. Chem., Int. Ed.* **2014**, *53*, 10330.
- (28) Ye, Y. D.; Sanford, M. S. *J. Am. Chem. Soc.* **2013**, *135*, 4648.
- (29) Zhang, C. W.; Li, Z. D.; Zhu, L.; Yu, L. M.; Wang, Z. T.; Li, C. Z. *J. Am. Chem. Soc.* **2013**, *135*, 14082.
- (30) Bloom, S.; Pitts, C. R.; Miller, D. C.; Haselton, N.; Holl, M. G.; Urheim, E.; Lectka, T. *Angew. Chem., Int. Ed.* **2012**, *51*, 10580.
- (31) Furuya, T.; Benitez, D.; Tkatchouk, E.; Strom, A. E.; Tang, P.; Goddard, W. A.; Ritter, T. *J. Am. Chem. Soc.* **2010**, *132*, 3793.
- (32) Furuya, T.; Ritter, T. *J. Am. Chem. Soc.* **2008**, *130*, 10060.
- (33) Tang, P. P.; Furuya, T.; Ritter, T. *J. Am. Chem. Soc.* **2010**, *132*, 12150.

- (34) Furuya, T.; Strom, A. E.; Ritter, T. *J. Am. Chem. Soc.* **2009**, *131*, 1662.
- (35) Pitts, C. R.; Bloom, S.; Woltornist, R.; Auvenshine, D. J.; Ryzhkov, L. R.; Siegler, M. A.; Lectka, T. *J. Am. Chem. Soc.* **2014**, *136*, 9780.
- (36) Hull, K. L.; Anani, W. Q.; Sanford, M. S. *J. Am. Chem. Soc.* **2006**, *128*, 7134.
- (37) Wang, X.; Mei, T.-S.; Yu, J.-Q. *J. Am. Chem. Soc.* **2009**, *131*, 7520.
- (38) Furuya, T.; Kaiser, H. M.; Ritter, T. *Angew. Chem., Int. Ed.* **2008**, *47*, 5993.
- (39) Chan, K. S. L.; Wasa, M.; Wang, X.; Yu, J.-Q. *Angew. Chem., Int. Ed.* **2011**, *50*, 9081.
- (40) Tang, P.; Ritter, T. *Tetrahedron* **2011**, *67*, 4449.
- (41) Huang, C. H.; Liang, T.; Harada, S.; Lee, E.; Ritter, T. *J. Am. Chem. Soc.* **2011**, *133*, 13308.
- (42) Furuya, T.; Ritter, T. *Org. Lett.* **2009**, *11*, 2860.
- (43) Campbell, M. G.; Ritter, T. *Chem. Rev.* **2015**, *115*, 612.
- (44) Milner, L. M.; Hall, L. M.; Lynam, J. M.; Slattery, J. M.; Pridmore, N. E.; Skeats, M. K.; Whitwood, A. C. Manuscript in preparation.
- (45) Johnson, D. G.; Lynam, J. M.; Mistry, N. S.; Slattery, J. M.; Thatcher, R. J.; Whitwood, A. C. *J. Am. Chem. Soc.* **2013**, *135*, 2222–2234.
- (46) Hartwig, J. *Organotransition Metal Chemistry from Bonding to Catalysis*; University Science Books: Sausalito, CA, 2010.
- (47) Barthazy, P.; Hintermann, L.; Stoop, R. M.; Worle, M.; Mezzetti, A.; Togni, A. *Helv. Chim. Acta* **1999**, *82*, 2448.
- (48) Coleman, K. S.; Holloway, J. H.; Hope, E. G. *J. Chem. Soc., Dalton Trans.* **1997**, 1713.
- (49) Brewer, S. A.; Coleman, K. S.; Fawcett, J.; Holloway, J. H.; Hope, E. G.; Russell, D. R.; Watson, P. G. *J. Chem. Soc., Dalton Trans.* **1995**, 1073.
- (50) Caskey, S. R.; Stewart, M. H.; Ahn, Y. J.; Johnson, M. J. A.; Rowsell, J. L. C.; Kampf, J. W. *Organometallics* **2007**, *26*, 1912.
- (51) Nyffeler, P. T.; Duron, S. G.; Burkart, M. D.; Vincent, S. P.; Wong, C. H. *Angew. Chem., Int. Ed.* **2005**, *44*, 192.
- (52) Ling, L.; Liu, K.; Li, X. Q.; Li, Y. X. *ACS Catal.* **2015**, *5*, 2458.
- (53) Castro-Rodrigo, R.; Esteruelas, M. A.; Fuertes, S.; Lopez, A. M.; Mozo, S.; Onate, E. *Organometallics* **2009**, *28*, 5941.
- (54) Cowley, M. J.; Lynam, J. M.; Slattery, J. M. *Dalton Trans.* **2008**, 4552.
- (55) Ahlrichs, R.; Bar, M.; Haser, M.; Horn, H.; Kolmel, C. *Chem. Phys. Lett.* **1989**, *162*, 165.
- (56) Schafer, A.; Klamt, A.; Sattel, D.; Lohrenz, J. C. W.; Eckert, F. *Phys. Chem. Chem. Phys.* **2000**, *2*, 2187.
- (57) Grimme, S.; Antony, J.; Ehrlich, S.; Krieg, H. *J. Chem. Phys.* **2010**, *132*, 154104.
- (58) Grimme, S.; Ehrlich, S.; Goerigk, L. *J. Comput. Chem.* **2011**, *32*, 1456.